



Delft University of Technology

**Direct air capture of CO<sub>2</sub> with an amine resin**  
**A molecular modeling study of the oxidative deactivation mechanism with O<sub>2</sub>**

Buijs, Wim

**DOI**

[10.1021/acs.iecr.9b03823](https://doi.org/10.1021/acs.iecr.9b03823)

**Publication date**

2019

**Document Version**

Final published version

**Published in**

Industrial and Engineering Chemistry Research

**Citation (APA)**

Buijs, W. (2019). Direct air capture of CO<sub>2</sub> with an amine resin: A molecular modeling study of the oxidative deactivation mechanism with O<sub>2</sub>. *Industrial and Engineering Chemistry Research*, 58(38), 17760-17767. <https://doi.org/10.1021/acs.iecr.9b03823>

**Important note**

To cite this publication, please use the final published version (if applicable).  
Please check the document version above.

**Copyright**

Other than for strictly personal use, it is not permitted to download, forward or distribute the text or part of it, without the consent of the author(s) and/or copyright holder(s), unless the work is under an open content license such as Creative Commons.

**Takedown policy**

Please contact us and provide details if you believe this document breaches copyrights.  
We will remove access to the work immediately and investigate your claim.

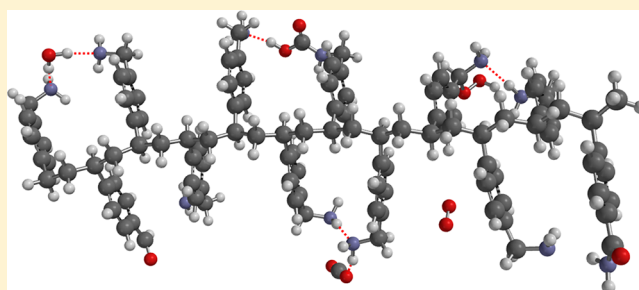
# Direct Air Capture of CO<sub>2</sub> with an Amine Resin: A Molecular Modeling Study of the Oxidative Deactivation Mechanism with O<sub>2</sub>

Wim Buijs\*

Process & Energy Department, Faculty of Mechanical, Maritime and Materials Engineering, Delft University of Technology, Leeghwaterstraat 39, 2628CB Delft, The Netherlands

## Supporting Information

**ABSTRACT:** Lewatit R VP OC 1065 is a promising material for direct air capture of CO<sub>2</sub>. However, it was found that serious oxidative degradation already started from 80 °C. In this DFT study, oxidative degradation is described as a series of well-known reactions in air-oxidation chemistry. Oxidation of the resin starts with the formation of an  $\alpha$ -benzyl amino hydroperoxide. Thermal decomposition of the  $\alpha$ -benzyl amino hydroperoxide is the second step and leads eventually to the corresponding amide (R(C=O)NH<sub>2</sub>) and the half-aminal (RCH(OH)(NH<sub>2</sub>)). The half-aminal further solvolyzes predominantly to an aldehyde (RCHO). Both the amide and the aldehyde are responsible for the experimentally observed loss of CO<sub>2</sub> capacity as these groups are not able to capture CO<sub>2</sub>. The rate-determining step in oxidative degradation is usually the decomposition of the hydroperoxide, but in this case the formation of the  $\alpha$ -benzyl amino hydroperoxide cannot be excluded. The apparent contradiction between the results of Hallenbeck et al. and Yu et al. with respect to the oxygen content before and after exposure of the resin to air at high temperature is explained by the difference in H<sub>2</sub>O content before and after and oxygen incorporation by amide and aldehyde formation after exposure to air. The loss of nitrogen content on exposure to air at high temperature is explained by the formation of aldehydes.



## INTRODUCTION

In 2017, a molecular modeling study was reported wherein the CO<sub>2</sub> capturing reactions of the polymeric resin Lewatit R VP OC 1065 were unambiguously identified and quantitatively described.<sup>1</sup> Since 2012, this resin is being reported as a promising material for direct air capture of CO<sub>2</sub> (DAC CO<sub>2</sub>) with respect to CO<sub>2</sub> capacity, amount of H<sub>2</sub>O adsorption and energy requirements for regeneration.<sup>2</sup> However, already in 2013, the same research group<sup>3</sup> reported a major loss of amine groups upon prolonged exposure to air at 120 °C. Recently, Yu et al.<sup>4</sup> reported significant oxidative degradation already above 70 °C in air. In this molecular modeling study, the initial reaction of O<sub>2</sub> with the resin and various consecutive reactions of the primary products are studied. The results obtained are compared with the literature data on oxidative degradation and the data obtained in the first molecular modeling study<sup>1</sup> to quantitatively estimate its effect on the performance and lifetime of the resin under realistic atmospheric conditions.

## MOLECULAR MODELING

All molecular modeling studies were performed using Wave function's Spartan '18 suite.<sup>5</sup> Molecular Mechanics (MMFF) was used to explore the physisorption complexes of O<sub>2</sub> with the previously obtained model for Lewatit R VP OC 1065, the saturated dodecamer of 4-aminomethyl vinylbenzene.<sup>1</sup> The results obtained with Molecular Mechanics were used as starting structures for various quantum chemical calculations,

wherein physisorption and particularly chemical reactions were investigated further using the saturated trimer of 4-aminomethyl vinylbenzene as a model. Wherever possible even smaller models like benzyl amine complexes were used to explore the potentially wide range of possible reactions. All structures were fully optimized using density functional theory (DFT) B3LYP/6-31-G\*. Transition states were identified and characterized using their unique imaginary vibrational frequency.<sup>6</sup> Applying as much as possible, the concept of isodesmic reactions<sup>7</sup> to yield gross cancelation of methodological/code errors, all reaction enthalpies and activation barriers were calculated using total energies and enthalpy corrections. Computational entropy corrections were not used because of the huge simplifications of the QM-systems. For reactions wherein it is very likely that molecules like H<sub>2</sub>O and NH<sub>3</sub> will escape to the gas phase, an entropy correction ( $T\Delta S$ ) based on the experimentally known  $\Delta S_{\text{vap}}$  of H<sub>2</sub>O and NH<sub>3</sub> was applied.<sup>8,9</sup> Quantitative results of all calculations (xlsx) and all molecular (ensemble) structures (zip) together with a small guidance document (pdf) are available in the Supporting Information.

**Received:** July 13, 2019

**Revised:** August 27, 2019

**Accepted:** August 28, 2019

**Published:** August 28, 2019

## RESULTS AND DISCUSSION

**Air Oxidation Chemistry.** Air oxidation is a chemical process with a considerable activation barrier because the ground state of  $O_2$  contains two unpaired electrons and is in the triplet state (t) while most substrates do not have unpaired electrons and are in the singlet state (s). Reactions between a triplet and a singlet state are so-called “forbidden” and not directly possible. Direct oxidation with air usually proceeds via a so-called free radical chain autoxidation (FRCA) process,<sup>10</sup> wherein the singlet substrate is converted into a species with an unpaired electron. The formation of a substrate radical with one unpaired electron usually requires an initiator. As an initiator, a peroxide (ROOH, ROOR) or high valent transition metal ion can act. The description “Autoxidation” in FRCA now becomes clear as (hydro)peroxides are usually the first detectable oxidation products. The importance of the presence of an initiator for oxidative degradation of the polyethyleneimine (PEI) resin at 110 °C was shown by Min et al.:<sup>11</sup> the removal of Fe- and Cu-ions (oxidation initiators) with chelating agents lead to a 50 times slower oxidative degradation. After initiation, the substrate radical easily can combine with dioxygen to form a peroxy radical (ROO•) which can extract an H atom from a substrate molecule to form a new radical (R•) and ROOH. This process is called propagation and creates the “chain”. Next ROOH formed can easily break up according to  $ROOH \rightarrow RO\cdot + HO\cdot$ , thus acting as an initiator itself and creating more radicals leading to “autoxidation”. The decomposition of ROOH (or ROOR) is usually the rate-determining step in air oxidation processes. The process is stopped by the coupling of two radicals, creating a singlet molecule (termination) which cannot further react with the triplet dioxygen.

**Literature Results on Oxidative Degradation of Lewatit R VP OC 1065 by  $O_2$ .** Oxidative degradation of Lewatit R VP OC 1065 in air has been reported by Hallenbeck and Kitchin<sup>3</sup> and by Yu et al.<sup>4</sup> In 2013, Hallenbeck and Kitchin found a reduction of 79%  $CO_2$  uptake and evidence for amine loss upon 7 days exposure to 120 °C in air. In 2017 Yu et al. reported a reduction of ~80%  $CO_2$  uptake upon 3 days exposure at 120 °C in air. Though both studies were meant merely as explorative studies, and not as kinetic or mechanistic studies, still remarkable differences can be observed apart from the apparent agreement on a reduction of ~80%  $CO_2$  uptake upon exposure to 120 °C in air:

(1) Based on elemental analysis, Hallenbeck and Kitchin concluded that oxidative degradation leads to deamination without increase of the oxygen content in the resin.

(2) Based on elemental analysis, Yu et al., observed a marked increase of the oxygen content in the resin.

A summary of both results is listed in Table 1 and will be discussed below.

The elemental analysis of the fresh sample of Hallenbeck et al. corresponds to a Lewatit R VP OC 1065, wherein ~67% of all active sites contain one  $H_2O$  molecule as shown in Figure 2, type 2. The value of ~67% coincides remarkably well with the partition of the two active sites previously obtained.<sup>1</sup> The fresh sample of Yu et al. contains only ~25% of type 2 active sites and as a consequence ~75% of type 1 active sites as shown in Figure 2. Thus, as the observed differences in oxygen content of the fresh resins can be explained satisfactorily as different amounts of  $H_2O$  in the resins, due to slightly different

**Table 1. Elemental Analysis of Lewatit R VP OC 1065 Samples before and after Exposure to 120 °C in Air<sup>a</sup>**

sample	% C	% H	% N	% O	% sum	N-loading (mol/kg)
fresh <sup>3</sup>	81.57	8.18	7.92	3.74	101.41	5.90
degraded <sup>3</sup>	81.8	7.4	6.4	4.0	99.6	4.77 <sup>b</sup>
fresh <sup>4</sup>	80.70	8.30	9.54	1.46	100.00	6.82
degraded <sup>4</sup>	79.53	7.00	7.35	6.12	100.00	5.25

<sup>a</sup>Average data from Hallenbeck and Kitchin<sup>3</sup> and Yu et al.<sup>4</sup>

<sup>b</sup>Recalculation from % N and starting N-loading.

experimental conditions, oxidative degradation on both sites will be investigated.

In addition, from the results of Yu et al.,<sup>4</sup> a rough estimate of the activation barrier can be obtained from the start of the reaction at 80 °C. Assuming that the oxidation of Lewatit R VP OC 1065 at the surface of the resin particles initially is not seriously hindered by mass transfer limitation, the overall reaction rate can be expressed as a pseudo first order reaction with  $k = k_0 e^{-E_a/RT}$  where  $k_0 = k_B T/h = \sim 6.2 \times 10^{12} s^{-1}$  at 298 K. At 80 °C, a loss of ~20%  $CO_2$  capacity (oxidative degradation) was observed in 12 h. Substituting all data in the rate expression results in an estimate for  $E_a$  of ~122.7 kJ/mol for oxidative degradation of Lewatit R VP OC 1065. Unfortunately the data of Hallenbeck et al. are not suited for this approach as they are available only at the highest temperature (120 °C) and an exposure time of 7 days only.

**Computational Results.** To ease the understanding and reasoning in this article, the previously obtained structure of Lewatit R VP OC 1065, poly *p*-vinyl benzyl amine, is evaluated shortly. For those readers with a keen interest in the elucidation of the structure of Lewatit R VP OC 1065, it is advised to read the first article in this series on DAC of  $CO_2$  with an amine resin where this is discussed in detail.<sup>1</sup> Figure 1 shows the structure obtained with Molecular Mechanics (MMFF) of the dodecamer of *p*-vinyl benzyl amine, using two different displays for reasons of clarity. In the resin, the

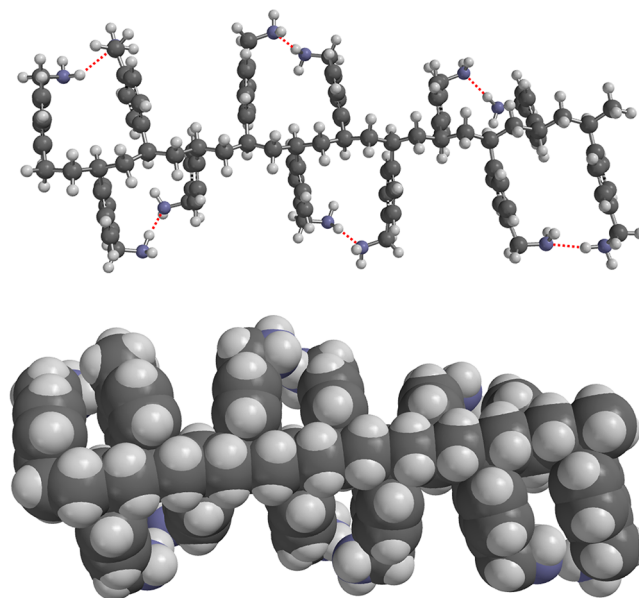


**Figure 1.** MMFF-structure of the dodecamer of *p*-vinyl benzyl amine. Atoms are displayed as ball and spoke or space filling. Hydrogen bridges are indicated by red dotted lines.

benzyl amine groups are orientated perpendicular to the polyvinyl backbone in an alternating mode, wherein all even (and odd) benzyl amine groups are within close vicinity. Both hydrogen bridging and  $\pi$ -stacking contribute to the stability as can be seen from the ball and spoke display. Rotational barriers of the Ar–CH<sub>2</sub>NH<sub>2</sub> bond of the benzyl amino groups over 180 deg are <10 kJ/mol, which means that all (alternating) benzyl amino groups will “see” each other continuously at or above room temperature.

The two benzylic positions in the Lewatit R VP OC 1065 resin are electronically most easily oxidized but the benzylic position in the polymer backbone is completely shielded as can be seen particularly well from the space filling display in Figure 1. The benzyl amino groups are accessible for oxidation and electronically strongly activated by the amino function. However, during exposure to air, CO<sub>2</sub> is captured by the benzyl amino groups to yield the corresponding carbamic acid. Two closely related types of active sites on the resin were identified for the CO<sub>2</sub> capturing reaction.<sup>1</sup> Type 1 active sites are built from just two alternating benzyl amino groups in the resin in close vicinity of each other. Type 2 sites are the result of strong physisorption of one molecule of H<sub>2</sub>O on two such alternating benzyl amino groups via H-bridging. Figure 2 shows the QM-models of the two types of active sites.

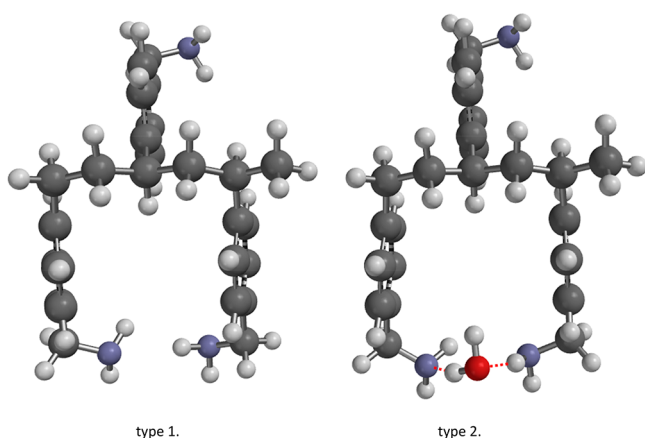


**Figure 2.** QM-models of the two active site models for CO<sub>2</sub> capturing of Lewatit R VP OC 1065. Atoms displayed as ball and spoke. Hydrogen bridges are indicated by red dotted lines.

Under atmospheric conditions with a CO<sub>2</sub> level of approximately 400 ppm, only one CO<sub>2</sub> is captured *per pair* of benzyl amino groups. Thus direct oxidation of the benzyl amino group, the benzyl carbamic acid group, and the benzyl amino group with a hydrogen bridge toward the benzyl carbamic acid group with O<sub>2</sub>(t) will be investigated for both types of active sites.

Oxidation starts with physisorption of O<sub>2</sub> to the resin. Figure 3 shows relevant parts of the types 1 and 2-O<sub>2</sub>(t) complexes. The MMFF-interaction energy for both types of active sites is about –2.5 kJ/mol. The (B3LYP/6-31G\*) interaction energy of O<sub>2</sub>(t) with the above-mentioned complexes ranges from –4.9 to –3.7 kJ/mol for types 1 and 2, respectively. The slightly larger stabilization energy of the active site type 1-O<sub>2</sub> complex is due to some spin coupling between O<sub>2</sub>(t) and an amino group as can be seen in Figure 3.

Now MMFF has an explicit description of the van der Waals energy<sup>12</sup> and should be trusted more from an accurate energy

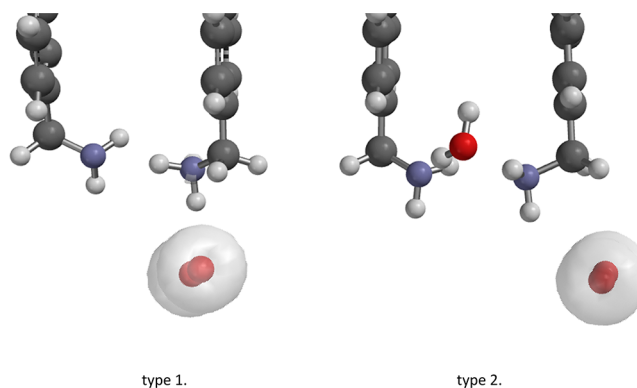


**Figure 3.** Details of the active site type 1 and 2-O<sub>2</sub>(t) physisorption complexes (B3LYP/6-31G\*; spin density, 0.002 e/au<sup>3</sup> as a transparent gray cloud). Atoms are displayed as ball and spoke.

point of view. Standard DFT like B3LYP/6-31G\* usually underestimates the dispersive part of the van der Waals interaction energy due to its time independent character, but in this case not. There are ongoing attempts to partly (re)-parametrize various DFT codes<sup>13,14</sup> to yield more accurate results; however, there is a lack of experimental data for larger systems to calibrate with. Important for this study is that B3LYP/6-31G\* energies will be used for all energy comparisons, including activation barriers.

The interaction energy of CO<sub>2</sub> with the resin yielded approximately –19.5 kJ/mol.<sup>1</sup> Surprisingly, the average difference in physisorption energy between CO<sub>2</sub> and O<sub>2</sub> ( $\Delta E = -19.5 - -4.5$  kJ/mol = –15.0 kJ/mol) and the difference in concentration (21% O<sub>2</sub> vs 400 ppm of CO<sub>2</sub>) leads to an approximately similar occupation of the resin with O<sub>2</sub> and CO<sub>2</sub> at room temperature:

$$\begin{aligned} e^{-\Delta E/RT} &= e^{-15.000/8.314 \times 298} = 426 \text{ and } [\text{O}_2]_g/[\text{CO}_2]_g \\ &= 210\,000/400 = 525 \rightarrow [\text{O}_2]_{\text{resin}}/[\text{CO}_2]_{\text{resin}} \\ &= 525/426 = 1.2 \end{aligned}$$

At increasing temperature, the  $[\text{O}_2]_{\text{resin}}/[\text{CO}_2]_{\text{resin}}$  increases to 3.2 at 80 °C and 5.3 at 120 °C.

The previously used equation for the overall reaction rate as a pseudo first order reaction (with  $k = k_0 e^{-E_a/RT}$  wherein  $k_0 = k_B T/h = \sim 6.2 \times 10^{12} \text{ s}^{-1}$  at 298 K) can also be used to estimate the ratio of the reaction rates for CO<sub>2</sub> capturing reactions and oxidative degradation. Apart from the earlier reported<sup>1</sup> activation barriers for the two CO<sub>2</sub> capturing reactions, 75.9 and 44.3 kJ/mol for types 1 and 2, respectively, and the estimate for oxidative degradation from Yu et al.<sup>4</sup> of 122.7 kJ/mol, the  $[\text{O}_2]_{\text{resin}}/[\text{CO}_2]_{\text{resin}}$  as a function of temperature as described above was used. Finally, it is assumed that the small difference in diffusion coefficients in water of O<sub>2</sub> ( $D_{\text{O}_2} = 2.1 \times 10^{-9} \text{ m}^2/\text{s}$ ) and CO<sub>2</sub> ( $D_{\text{CO}_2} = 1.9 \times 10^{-9} \text{ m}^2/\text{s}$ )<sup>23</sup> will be reflected in the resin as a diffusion medium. Table 2 lists the results for type 1 and 2 sites at 25 and 80 °C.

**Table 2.** Ratio CO<sub>2</sub> Capturing Reactions/Oxidative Degradation for Lewatit R VP OC 1065 at 25 °C and 80 °C

$r\text{-CO}_2/r\text{-O}_2$	25 °C	80 °C
type 1	$1.59 \times 10^7$	$4.52 \times 10^5$
type 2	$3.27 \times 10^{10}$	$2.83 \times 10^8$



From Table 2, it is clear that the two CO<sub>2</sub> capturing reactions in all cases are much faster than the oxidation reaction, although there is a marked influence of type of active site and temperature. Thus, the products of the CO<sub>2</sub> capturing reactions should be considered in the possible options for oxidative degradation too. This leads to six possible options for the direct reaction of O<sub>2</sub>(t) with the resin using the trimeric model as listed in Table 3. Figure 4 shows the transition state

**Table 3. Overview Activation Barriers and Unique Imaginary Frequencies ( $\nu$ ) of H-Atom Transfer Reactions (B3LYP/6-31G\*)**

system: trimer		active site type	$E_a$ (kJ/mol)	$\nu$ (cm <sup>-1</sup> )
functional groups on active site				
benzyl amino	benzyl amino	1	117.5	i1219
		2	109.0	i1337
benzyl amino	benzyl carbamic acid	1	133.1	i1011
		2	128.2	i1302
benzyl carbamic acid	benzyl amino	1	150.7	i1284
		2	153.1	i811

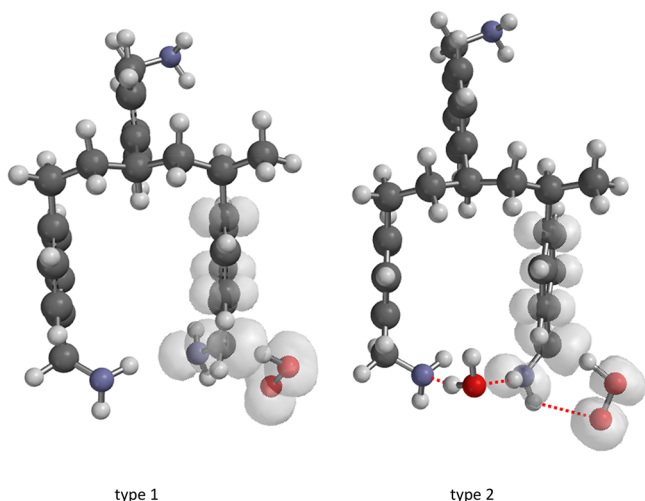


**Figure 4.** Transition state of the H atom transfer from a benzyl amino group to O<sub>2</sub>(t) for the two types of active sites. B3LYP/6-31G\* (spin density, 0.002 e/au<sup>3</sup> as a transparent gray cloud). Atoms displayed as balls and spokes. Hydrogen bridges are indicated by red dotted lines.

for H atom transfer from the benzylic C to the O of O<sub>2</sub>(t) for the two types of active sites. On animation, the unique imaginary frequency ( $\nu$ ) shows the expected movement. From the spin density, the stabilization of the benzylic radical both from the aromatic nucleus and the amino group is clearly visible.

The activation barriers for all possible H-transfer reactions range from 109.0 kJ/mol for a benzyl amino group in a type 2 active site to 153.1 kJ/mol for a carbamic acid group from a type 1 active site. Most of the barriers are much lower as for toluene with the exception of the cases wherein the carbamic acid group is next to the benzylic CH<sub>2</sub> which show activation barriers close to the activation barrier of 160.6 kJ/mol for toluene, in line with the starting temperature of the noncatalyzed air oxidation of toluene at ~180 °C.<sup>7</sup> The formation of a carbamic acid from an amine also greatly reduces the sensibility for oxidation of a benzyl amino group that is connected via a hydrogen bridge with the carbamic acid

group formed. In addition H<sub>2</sub>O, via a type 2 active site, should be considered as an effective protection against oxidative degradation. These results are in line with the experimental findings of Heydari-Gorji et al.,<sup>24</sup> for polyethylene-imine resins and Yu et al.,<sup>4</sup> both reporting the oxidation inhibiting effect of CO<sub>2</sub> and H<sub>2</sub>O.

Inspecting Table 3 leads to the conclusion that only the original resin itself, represented by the trimers of types 1 and 2 active sites provide suitable candidates, benzyl amino groups, for oxidative degradation as both activation barriers are <122.7 kJ/mol. Type 2 active site shows the lowest activation barrier for the initial oxidative degradation but also the fastest reaction toward the carbamic acid, providing protection against oxidation. For type 1 active sites, a similar situation exists albeit not as outspoken as for type 2 sites.

Now rotation of a benzyl amino group bridged to a benzyl carbamic acid would lead to a situation wherein the benzyl carbamic acid group is (temporarily) left alone with or without a molecule of H<sub>2</sub>O, depending on the type of active site considered, while at the same time a new active site type 1 can be formed with two benzyl amino groups. Therefore, the energy profiles of the rotation of benzyl amino groups with different neighboring groups (benzyl amino and H<sub>2</sub>O, benzyl carbamic acid, benzyl carbamic acid, and H<sub>2</sub>O) were investigated using Molecular Mechanics (MMFF).

Rotation of a benzyl amino group of a type 2 active site yields a type 1 active site and a single benzyl amino group with a H-bridge to H<sub>2</sub>O. The rotational barrier is 27.0 kJ/mol. At room temperature, the stabilization energy of H<sub>2</sub>O in the original type active site is -22.4 kJ/mol, as the result of an enthalpy gain of -54.9 kJ/mol (H-bridges) and an entropy gain of 32.5 kJ/mol ( $T\Delta S_{\text{vap}}$  at 298 K). Thus, rotation of a benzyl amino group in a type 2 active site will lead to a type 1 active site, while the remaining H<sub>2</sub>O becomes mobile and might escape to the gas phase. Thus, the complexation energy of H<sub>2</sub>O can be considered as the activation barrier for the removal of H<sub>2</sub>O from a type 2 active site while creating a type 1 active site. That barrier is still ~20 kJ/mol lower than the activation barrier for carbamic acid formation and thus will occur much faster.

Rotation of a benzyl amino group next to a benzyl carbamic acid group leads to the formation of a type 1 active site and a single benzyl carbamic acid. The process is slightly endothermic. The rotational barrier is 38.0 kJ/mol so it is still a fast process compared to carbamic acid formation on a type 1 active site which has an activation barrier of 75.9 kJ/mol. Finally, rotation of a benzyl amino group from a benzyl carbamic acid-H<sub>2</sub>O-benzyl amino group site yields a type 1 active site and a benzyl carbamic acid with a H-bridge to H<sub>2</sub>O. The rotational barrier is 48.0 kJ/mol. At room temperature the stabilization energy of H<sub>2</sub>O in this case is -24.0 kJ/mol as the sum of an enthalpy gain of -56.5 kJ/mol and an entropy gain of 32.5 kJ/mol. Thus, H<sub>2</sub>O will be easily removed in this process too.

Summarizing the results presented above, the formation of a type 1 active site from an original type 2 active site, a benzyl carbamic acid-benzyl amino complex or a benzyl carbamic acid-H<sub>2</sub>O-benzyl amino complex, is a fast process compared to carbamic acid formation itself and leads to the removal of H<sub>2</sub>O if present in the starting complex. With respect to the initial step in oxidative degradation of the resin, it means that H atom transfer from a benzyl amino group to the O<sub>2</sub>(t) in a

type 1 active site with an activation barrier of 117.5 kJ/mol is the most likely candidate.

The products of that reaction are an amino benzyl radical ( $\text{ArCHNH}_2(\text{d})$ ) and  $\text{HO}_2(\text{d})$ . As the amount of  $\text{O}_2$  is abundant, the amino benzyl radical will react in a barrier free process with a second  $\text{O}_2(\text{t})$  molecule to yield an amino-benzylperoxy radical ( $\text{ArCH}(\text{NH}_2)\text{O}_2(\text{d})$ ). Propagation of the oxidation chain in Lewatit R VP OC 1065 should occur via relatively small species, like  $\text{O}_2(\text{t})$ ,  $\text{HO}_2(\text{d})$ , and  $\text{OH}(\text{d})$ , as the mobility of the polymeric backbone is limited and attack of the amino-benzylperoxy radical on the neighboring benzyl amino group will show a considerable activation barrier because of the loss of the hydrogen bridges between the various amino groups and  $\text{H}_2\text{O}$  in type 1 and 2 sites.

The  $\text{HO}_2$  radical formed in the initiating step reacts essentially barrier free with the  $\alpha$ -amino benzyl peroxy radical to yield the corresponding  $\alpha$ -amino-benzyl hydroperoxide and  $\text{O}_2(\text{t})$ . This was confirmed by using a smaller system,  $\text{ArCH}(\text{NH}_2)\text{O}_2$  and  $\text{HO}_2(\text{t})$  which yielded  $\text{ArCH}(\text{NH}_2)\text{O}_2\text{H}$  and  $\text{O}_2(\text{t})$  with an activation barrier of 3.3 kJ/mol. Alternatively, the amino benzyl radical might combine directly with the  $\text{HO}_2$  radical to yield the  $\alpha$ -amino-benzyl hydroperoxide and  $\text{O}_2(\text{t})$ , but this requires a intersystem crossing which is a rather slow process.<sup>15</sup>

The structures of the two  $\alpha$ -amino-benzyl hydroperoxides are shown in Figure 5. Type 1 shows two H-bridges, while type

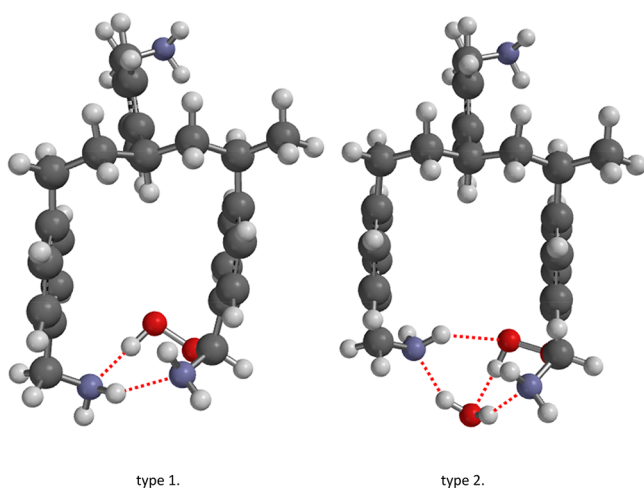


**Figure 5.** B3LYP/6-31G\* structures of  $\alpha$ -amino-benzyl hydroperoxides of type 1 and type 2 sites. Atoms displayed as ball and spoke. Hydrogen bridges are indicated by red dotted lines.

2 shows four H-bridges. There is no significant difference between the reaction enthalpies of the formation of the  $\alpha$ -amino-benzyl hydroperoxides as they are  $-76.2$  and  $-74.9$  kJ/mol for types 1 and 2, respectively.

As mentioned before, hydroperoxides do undergo thermal decomposition easily. Thermal decomposition of cumyl hydroperoxide shows an activation barrier of  $122.0 \pm 3$  kJ/mol.<sup>16</sup> The previously made estimate for the activation barrier of 122.7 kJ/mol for oxidative degradation of Lewatit R VP OC 1065 coincides quite well with this value as well as the activation barrier of 117.5 kJ/mol for H atom transfer from the benzyl amino group to  $\text{O}_2(\text{t})$ . So it can be concluded that either thermal decomposition of the  $\alpha$ -amino-benzyl hydroperoxide or H atom transfer from the benzyl amino group to

$\text{O}_2(\text{t})$  is the rate-determining step in the oxidative degradation of Lewatit R VP OC 1065.

Homolytic splitting of the O–O bond leads to two very reactive radicals, the  $\alpha$ -amino benzyloxy radical and the OH radical. The OH radical is an extremely reactive electrophilic species,<sup>17</sup> which shows at room temperature both H atom abstraction from the aromatic side chain and radical addition to aromatic nuclei.<sup>18,19</sup> Using benzyl amine and the OH radical as a much smaller system, activation barriers of 11.4 ( $\nu = \text{i}193 \text{ cm}^{-1}$ ) and 11.6 kJ/mol ( $\nu = \text{i}302 \text{ cm}^{-1}$ ) were obtained for H-abstraction and radical addition, respectively, in line with the above-mentioned experimental findings. As there are six accessible aromatic and two accessible benzylic sites, it can be expected that the OH radical will contribute only to a minor extent to chain propagation, while still leading to other oxidative damage of Lewatit R VP OC 1065. The  $\alpha$ -amino benzyloxy radical can undergo two reactions:

(1) The  $\alpha$ -amino benzyloxy radical loses a hydrogen atom via H atom abstraction by  $\text{O}_2(\text{t})$  to yield the corresponding amide  $\text{ArCONH}_2$  ( $E_a$  type 1 = 10.0 kJ/mol;  $\nu = \text{i}604 \text{ cm}^{-1}$ ;  $\Delta H$  type 1 =  $-399.9$  kJ/mol and  $E_a$  type 2 = 1.2 kJ/mol;  $\nu = \text{i}195 \text{ cm}^{-1}$ ;  $\Delta H$  type 2 =  $-384.0$  kJ/mol). However, both type 1 and 2 sites easily will lose 1 and 2 molecules of  $\text{H}_2\text{O}$  to the gas phase, respectively, as the gain in enthalpy is equal to  $T\Delta S_{\text{vap}}$  of  $\text{H}_2\text{O}$  at 80 °C. After removal of  $\text{H}_2\text{O}$ , the formation of an amide shows a  $\Delta H = -361.8$  kJ/mol for both type sites.

(2) The  $\alpha$ -amino benzyloxy radical abstracts a hydrogen atom from  $\text{HO}_2\cdot$  to yield the corresponding half-aminal  $\text{R-ArCH}(\text{OH})(\text{NH}_2)$  ( $E_a$  type 1 = 39.9 kJ/mol;  $\nu = \text{i}46 \text{ cm}^{-1}$ ;  $\Delta H$  type 1 =  $-163.1$  kJ/mol and  $E_a$  type 2 = 18.2 kJ/mol;  $\nu = \text{i}31 \text{ cm}^{-1}$ ;  $\Delta H$  type 2 =  $-161.2$  kJ/mol).

Thus, the computational results show low barrier processes for both reactions. Despite the very low imaginary frequencies of the transition states, they do show the expected movement on animation. The final ratio of the two products depends on the local concentrations of the  $\text{HO}_2$  radical and  $\text{O}_2(\text{t})$  too. As  $\text{O}_2(\text{t})$  is far more abundant as the  $\text{HO}_2$  radical, formation of the amide will be favored over formation of the half-aminal. The loss of  $\text{H}_2\text{O}$  from amide complexes offers an attractive explanation for the difference in experimental observations between Hallenbeck<sup>3</sup> and Yu.<sup>4</sup> Starting from a resin with ~67% of type 2 active sites (Hallenbeck), containing one  $\text{H}_2\text{O}$  molecule, formation of an amide will not lead to an increase of oxygen content as the  $\text{H}_2\text{O}$  molecules from these sites will escape to the gas phase. On the other hand, starting from a resin with 75% of type 1 sites (Yu), formation of an amide will lead to a marked increase of the oxygen content. The structures of both products on both sites are shown in Figure 6.

Half-aminals are known as reactive intermediates in solution and undergo solvolysis to either an aldehyde or an imine, depending on the structure and the relative amounts of amine and  $\text{H}_2\text{O}$ .<sup>20</sup> From the patents<sup>21,22</sup> describing a reductive amination process, it is clear that a molar ratio  $\text{NH}_3/\text{RCHO} > 10$  is required to obtain >85% yield to a primary amine, originating from the corresponding imine. In type 1 active sites, no  $\text{H}_2\text{O}$  is present but one  $\text{RNH}_2$  is, while in type 2 active sites 1  $\text{H}_2\text{O}$  and 1  $\text{RNH}_2$  are present. Thus, a type 1 site reflects a situation wherein  $\text{NH}_3/\text{RCHO} = 2/1$  and type 2  $\text{NH}_3/\text{RCHO} = 2/2$ , both of them in favor of aldehyde formation.

Figure 7 shows the transition states for the formation of the aldehyde from the half-aminal of the two active site models.

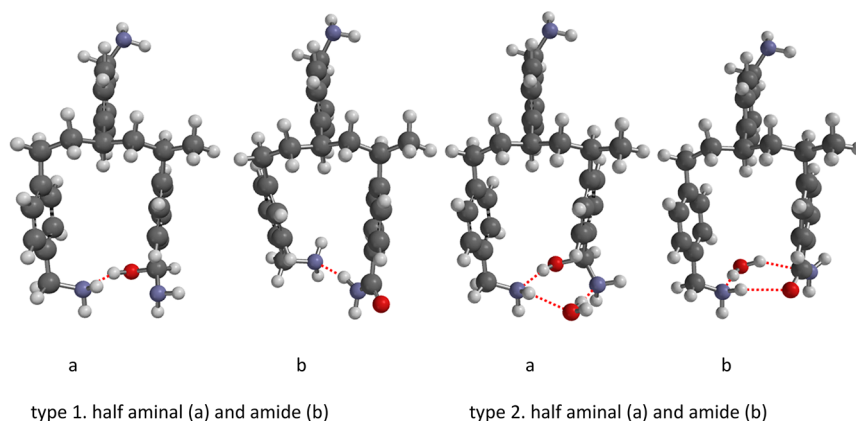


**Figure 6.** B3LYP/6-31G\* primary products of the thermal decay of the  $\alpha$ -amino-benzyl hydroperoxide of the two active site models. Atoms are displayed as ball and spoke. Hydrogen bridges are indicated by red dotted lines.

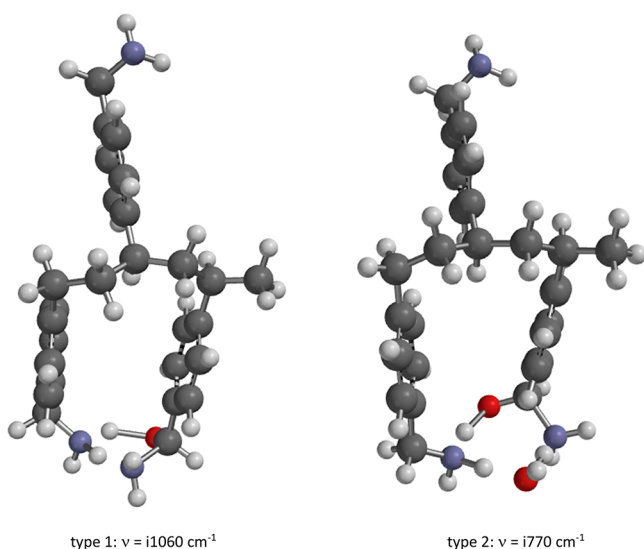


**Figure 7.** B3LYP/6-31G\* transition states of the aminolysis of the half-aminals originating from type 1 and type 2 sites with their unique imaginary frequencies ( $\nu$ ). Atoms are displayed as ball and spoke.

The activation barriers for this reaction are +101.6 kJ/mol and +84.2 kJ/mol, respectively, reflecting the difference in amine catalysis in type 1 sites and amine–H<sub>2</sub>O catalysis in type 2 sites. The reaction enthalpies ( $\Delta H$ ) for the formation of the aldehyde from the half-aminal of active site type 1 and type 2 are –4.8 and –7.9 kJ/mol, respectively. Release of NH<sub>3</sub> and NH<sub>3</sub> + H<sub>2</sub>O to the gas phase leads to an estimate for  $\Delta G$  of this reaction of –24.6 and –12.5 kJ/mol, respectively.

The reaction enthalpy for the formation of the imine from the half aminal for type 1 and type 2 sites is +10.1 and 9.2 kJ/mol, respectively. The forward activation barriers for this reaction are +155.8 kJ/mol and +149.8 kJ/mol, respectively. Both reaction energies and activation barriers make this reaction quite unlikely.

From the combined experimental and computational results, it can be concluded that aldehyde formation is strongly favored over imine formation. Furthermore, the formation of an aldehyde is accompanied by the release of NH<sub>3</sub> to the gas phase. This leads to a loss of nitrogen in the resin, which was indeed observed experimentally by Hallenbeck<sup>3</sup> and Yu,<sup>4</sup> showing a decrease of 1.1 mol/kg and 1.5 mol/kg of N-loading of the resin, respectively. This reaction also contributes to an

increase of the oxygen content of the resin which will be masked by the release of H<sub>2</sub>O to the gas phase on type 2 sites.

In solution, the presence of both aldehydes and amines will lead easily to the formation of imines and aminals; however, the mobility of the benzyl amine groups in Lewatit R VP OC 1065 is limited. Even the formation of a cyclic imine with a nearby amino group leads to considerable strain on top of unfavorable thermodynamics and kinetics.

**Final Discussion.** In this molecular modeling study, the experimentally observed oxidative degradation of Lewatit R VP OC 1065 is described as a series of well-known reactions from air-oxidation chemistry. Oxidative degradation of Lewatit R VP OC 1065 starts with the initial formation of  $\alpha$ -amino-benzyl hydroperoxides from starting benzyl amino groups and O<sub>2</sub>. Next follows the thermal decomposition of the  $\alpha$ -amino-benzyl hydroperoxide to yield sites no longer capable of capturing CO<sub>2</sub>. An estimate based on the experimental data of Yu et al.<sup>4</sup> for the overall activation barrier of oxidative degradation of the resin yielded 122.7 kJ/mol. This might very well be the activation barrier for decomposition of the  $\alpha$ -amino-benzyl hydroperoxide, as decomposition of the hydroperoxide usually is the rate-determining step in air oxidation chemistry. However, it cannot be excluded entirely that in this case the activation barrier of the initial formation of  $\alpha$ -amino-benzyl hydroperoxide (117.5 kJ/mol) is the rate-determining step. Unfortunately the activation barrier of the decomposition of the  $\alpha$ -amino-benzyl hydroperoxide itself cannot easily be determined as it depends largely on trace amounts of radical initiators like high valent metal ions, NO<sub>x</sub>, etc.<sup>11</sup> However, if the actual activation barrier for the decomposition of the  $\alpha$ -amino-benzyl hydroperoxide is higher than the activation barrier for the formation of the  $\alpha$ -amino-benzyl hydroperoxide, a serious safety risk might occur. To illustrate the risk only, a simple kinetic model, available in the [Supporting Information](#), was constructed based on two consecutive pseudo first order reactions:

(1) The formation of an  $\alpha$ -amino-benzyl hydroperoxide with  $E_a(1) = 117.5$  kJ/mol.

(2) The decomposition of the  $\alpha$ -amino-benzyl hydroperoxide with  $E_a(2) = 120.0$  kJ/mol

This model yields a loss of CO<sub>2</sub> capacity of 20.1% in 12 h at 80 °C, also in line with the work of Yu et al.,<sup>4</sup> while another 26.3% based on the total amount of benzyl amino groups, is left as the  $\alpha$ -amino-benzyl hydroperoxide. It should be noted that an active site containing an  $\alpha$ -amino-benzyl hydroperoxide



will still be able to capture CO<sub>2</sub>. Stretching the model to its other extreme with  $E_a(1) = 122.7$  kJ/mol (the experimental estimate) and  $E_a(2) = 109.0$  kJ/mol, still leads to 0.8% of  $\alpha$ -amino-benzyl hydroperoxide at a CO<sub>2</sub> capacity loss of 19.1%. While an absolute error in the B3LYP-derived activation barrier of 117.5 of  $\pm 5$  kJ/mol is plausible, an error of  $\pm 10$  kJ/mol is not. Once more it should be noted that for a serious chemical engineering model, dealing with simultaneous reaction, diffusion, and mass transfer limitation of multiple components, these calculated activation barriers should only serve as input. However, the latter requires an additional article and is a future perspective. In the meantime, it is strongly advised to experimental groups to perform some suitable peroxide testing on the resin after exposure to air particularly at temperatures  $>70$  °C. Anyway desorption of CO<sub>2</sub> in air at temperatures higher than room temperature should be avoided. Desorption of CO<sub>2</sub> in steam at 100 °C is advised to avoid any safety risk. Applying the same calculation with the original values for the activation barriers yields 0.034% of  $\alpha$ -amino-benzyl hydroperoxide in 12 h at 25 °C. The latter would indicate  $\sim 1500$  process cycles to reach 50% oxidative degradation, which might be enough from an economic point of view.

The primary products of the  $\alpha$ -amino-benzyl hydroperoxides are the corresponding amide (R(C=O)NH<sub>2</sub>) and the half a minal (RCH(OH)(NH<sub>2</sub>)). The half-aminal further solvolyzes predominantly to an aldehyde (RCHO). Both the amide and the aldehyde are responsible for the experimentally observed loss of CO<sub>2</sub> capacity as these groups are not able to capture CO<sub>2</sub>.

The apparent contradiction between the results of Hallenbeck<sup>3</sup> and Yu<sup>4</sup> on oxidative degradation of Lewatit R VP OC 1065 with respect to the oxygen content before and after exposure to air at high temperature is satisfactorily explained by the difference in H<sub>2</sub>O content before and after and oxygen incorporation by amide and aldehyde formation after exposure to air.

The loss of nitrogen content of Lewatit R VP OC 1065 on exposure to air at high temperature, observed both by Hallenbeck<sup>3</sup> and Yu,<sup>4</sup> is satisfactorily explained by the formation of aldehydes.

## ■ ASSOCIATED CONTENT

### ● Supporting Information

The Supporting Information is available free of charge on the ACS Publications website at DOI: 10.1021/acs.iecr.9b03823.

Guidance Supporting Information (PDF)

Molecular modelling data (XLSX)

All molecular structures [task name\_method.pdb] (ZIP)

## ■ AUTHOR INFORMATION

### Corresponding Author

\*E-mail: w.buijs@tudelft.nl

### ORCID

Wim Buijs: 0000-0003-3273-5063

### Notes

The author declares no competing financial interest.

## ■ REFERENCES

(1) Buijs, W.; de Flart, S. Direct Air Capture of CO<sub>2</sub> with an Amine Resin: A Molecular Modelling Study of the CO<sub>2</sub> Capturing Process. *Ind. Eng. Chem. Res.* **2017**, *56*, 12297–12304.

(2) Alesi, W. R., Jr.; Kitchin, J. R. Evaluation of a Primary Amine-Functionalized Ion-Exchange Resin for CO<sub>2</sub> Capture. *Ind. Eng. Chem. Res.* **2012**, *51*, 6907–6915.

(3) Hallenbeck, A. P.; Kitchin, J. R. Effects of O<sub>2</sub> and SO<sub>2</sub> on the Capture Capacity of a Primary-Amine Based Polymeric CO<sub>2</sub> Sorbent. *Ind. Eng. Chem. Res.* **2013**, *52* (31), 10788–10794.

(4) Yu, Q.; Delgado, J. d. I. P.; Veneman, R.; Brilman, D. W. F. Stability of a Benzyl Amine Based CO<sub>2</sub> Capture Adsorbent in View of Regeneration Strategies. *Ind. Eng. Chem. Res.* **2017**, *56*, 3259–3269.

(5) Wavefunction Inc. [www.wavefun.com](http://www.wavefun.com).

(6) Fukui, K. A Formulation of the Reaction Coordinate. *J. Phys. Chem.* **1970**, *74* (23), 4161–4163.

(7) Hehre, W. J.; Ditchfield, R.; Radom, L.; Pople, J. A. Molecular Orbital Theory of the Electronic Structure of Organic Compounds. V. Molecular Theory of Bond Separation. *J. Am. Chem. Soc.* **1970**, *92*, 4796.

(8) For FS<sub>vap</sub> water (H<sub>2</sub>O) see [http://www1.lsbu.ac.uk/water/water\\_properties.html](http://www1.lsbu.ac.uk/water/water_properties.html) accessed on August 26, 2019.

(9) For FS<sub>vap</sub> ammonia (NH<sub>3</sub>) see [https://www.engineeringtoolbox.com/ammonia-d\\_1413.html](https://www.engineeringtoolbox.com/ammonia-d_1413.html) accessed on August 26, 2019.

(10) Sheldon, R. A.; Kochi, J. *Metal-Catalyzed Oxidation of Organic Compounds*; Academic Press, Inc.: New York, 1981.

(11) Min, K.; Choi, W.; Kim, C.; Choi, M. Oxidation-stable amine-containing adsorbents for carbon dioxide capture. *Nat. Commun.* **2018**, *9*, 726.

(12) Halgren, T. A. MMFF VII. Characterization of MMFF94, MMFF94s, and Other Widely Available Force Fields for Conformational Energies and for Intermolecular-Interaction Energies and Geometries. *J. Comput. Chem.* **1999**, *20*, 730–748.

(13) Grimme, S.; Antony, J.; Ehrlich, S.; Krieg, H. A consistent and accurate ab initio parametrization of density functional dispersion correction (DFT-D) for the 94 elements H–Pu. *J. Chem. Phys.* **2010**, *132*, 154104.

(14) Smith, D. G. A.; Burns, L. A.; Patkowski, K.; Sherrill, C. D. Revised Damping Parameters for the D3 Dispersion Correction to Density Functional Theory. *J. Phys. Chem. Lett.* **2016**, *7*, 2197–2203.

(15) Gould, I. R.; Boiani, J. A.; Gaillard, E. B.; Goodman, J. L.; Farid, S. Intersystem Crossing in Charge-Transfer Excited States. *J. Phys. Chem. A* **2003**, *107* (18), 3515–3524.

(16) Duh, Y.-S.; Kao, C.-S.; Hwang, H.-H.; Lee, W.W.-L. *Process Saf. Environ. Prot.* **1998**, *76* (4), 271–276.

(17) Attri, P.; Kim, Y. H.; Park, D. H.; Park, J. H.; Hong, Y. J.; Uhm, H. S.; Kim, K.-N.; Fridman, A.; Choi, E. H. Generation mechanism of hydroxyl radical species and its lifetime prediction during the plasma-initiated ultraviolet (UV) photolysis. *Sci. Rep.* **2015**, *5*, 9332.

(18) Perry, R. A.; Atkinson, R.; Pitts, J. N., Jr. Kinetics and Mechanism of the Gas Phase Reaction of OH Radicals with Aromatic Hydrocarbons Over the Temperature Range 296–473 K. *J. Phys. Chem.* **1977**, *81* (4), 296–304.

(19) Mulder, P.; Louw, R. Gas Phase Reactions of Hydroxyl Radicals with Arenes. *Tetrahedron Lett.* **1982**, *23* (25), 2605–2608.

(20) Godoy-Alcantar, C.; Yatsimirsky, A. K.; Lehn, J.-M. Structure-stability correlations for imine formation in aqueous solution. *J. Phys. Org. Chem.* **2005**, *18*, 979–985.

(21) Buijs, W.; Wolters, H. F. W.; Lane, S. L.; Herkes, F. E.; Haasen, N. F. Preparation of *e*-caprolactam, and *e*-caprolactam precursors starting from 5-formylvalerate with less byproduct formation. Eur. Pat. Appl. EP 729943 A2 960904, EP 96-200499 960227, U.S. Pat. Appl. 95-396240 950301, 1996.

(22) Buijs, W.; Wolters, H. F. W. Preparation of *e*-caprolactam in high yield starting from 5-formylvaleric acid and derivatives. Eur. Pat. Appl. EP 729944 A2 960904, EP 96-200500 960227, U.S. Pat. Appl. 95-396240 950301, 1996.

(23) Diffusion coefficients of O<sub>2</sub> and CO<sub>2</sub>: The Engineering ToolBox. *Diffusion Coefficients of Gases in Water*, [https://www.engineeringtoolbox.com/diffusion-coefficients-d\\_1404.html](https://www.engineeringtoolbox.com/diffusion-coefficients-d_1404.html), accessed on August 26, 2019.



(24) Heydari-Gorji, A.; Sayari, A. Thermal, Oxidative, and CO<sub>2</sub>-Induced Degradation of Supported Polyethylenimine Adsorbents. *Ind. Eng. Chem. Res.* **2012**, *51*, 6887–6894.